Additivity of guest and host properties in clathrates: a thermodynamic and Raman spectroscopic investigation of HPTB-based solids

1996 J. Phys.: Condens. Matter 8 1647

(http://iopscience.iop.org/0953-8984/8/11/010)

J. Phys.: Condens. Matter **8** (1996) 1647–1661. Printed in the UK

Additivity of guest and host properties in clathrates: a thermodynamic and Raman spectroscopic investigation of HPTB-based solids

Darek Michalski, Randall T Perry and Mary Anne White†

Dalhousie University, Department of Chemistry, Halifax, Nova Scotia, Canada, B3H 4J3

Received 26 July 1995, in final form 16 November 1995

Abstract. The heat capacities of hexakis(phenylthio)benzene (abbreviated as HPTB) and the clathrate HPTB · $2CBr_4$ have been determined from 30 to about 300 K. In addition, the room-temperature Raman spectra have been obtained for both compounds. The Raman spectrum of HPTB·$2CBr_4$ is very closely approximated by the sum of the spectrum of HPTB and that of pure CBr_4, indicating the additivity of the guest and host intramolecular interactions. These internal degrees of freedom dominate the heat capacity, and the present analysis shows the importance of the low-frequency modes. Over a wide range of temperature below 200 K, the calculated Grüneisen parameter of HPTB is higher than for HPTB · $2CBr_4$.

1. Introduction

The term *inclusion compound* refers to materials in which one type of species (the 'guest') is spatially confined in cavities distributed within another species (the 'host') [1]. The host–guest interaction and/or the topology distinguish *clathrates* as lattice inclusion compounds in which the guest molecules are confined by steric barriers created by the architecture of a crystalline host framework [2, 3]. The interaction between the guest and host molecules in a clathrate is usually weak in comparison with covalent chemical bonding [4]. Therefore, to a first approximation, guest–host interactions can be neglected to give a simplified picture of two non-interacting subsystems (guests and hosts) [5, 6, 7], although recent molecular dynamics calculations have shown the significance of guest–host interactions for the physical properties of some clathrates [8, 9, 10]. The existence of many clathrates is due to the presence of guest molecules in voids of the host lattice. *Clathrands*, i.e. clathrates without guests, usually do not exist due to the instability of the empty isostructural host framework.

Since thermal and mechanical properties of materials are determined by intermolecular forces, clathrates offer an opportunity to probe the role of intermolecular interactions in the determination of physical properties. This is especially the case because different concentrations and types of guest species can be studied, often with little effect on the structure and dynamics of the host lattice.

Thermal properties of clathrates have been of particular interest. For example, the thermal conductivities of all clathrates that have been measured to date [11–16] exhibit temperature dependences similar to what is usually seen in glassy materials.

† Author to whom any correspondence should be addressed; email: MAWHITE@CHEM1.CHEM.DAL.CA.

0953-8984/96/111647+15$19.50

Other important related aspects include the melting behaviour of clathrates [17], the process of their formation and concomitant to that their thermodynamic stability; each relies on understanding thermal properties of the materials involved.

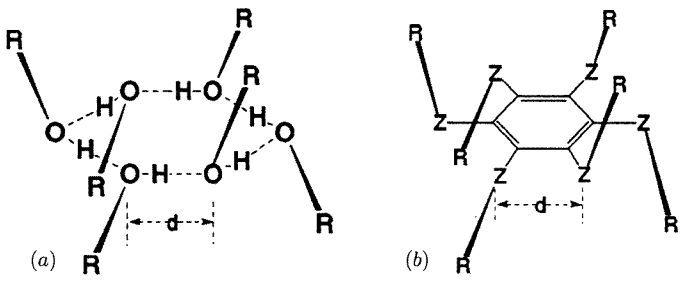

Figure 1. The similarity of (a) hexahost inclusion compound to (b) hexasubstituted benzene.

A new group of clathrates were designed and synthesized in the mid-1970s. The basis of the design of their host molecules came from the similarity of a hydrogen-bonded hexamer unit (e.g. as in Dianin's clathrate) with hexasubstituted benzene [18, 19] This resemblance is shown in figure 1. This system is one of the first examples of crystal engineering of a host lattice.

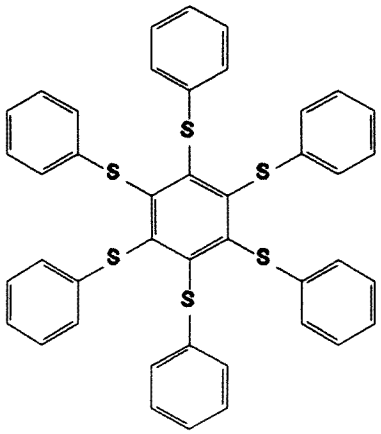

Figure 2. The molecular structure of hexakis(phenylthio)benzene, abbreviated as HPTB.

We report here thermodynamic and Raman spectroscopic findings for hexakis(phenylthio)benzene (figure 2; HPTB for short), the archetypal member of the family of hexasubstituted benzene clathrates. The clathrate investigated was HPTB · $2CBr_4$, and the thermal properties determined are compared herein with those of the molecular crystal, HPTB. The topology of this clathrate is slightly more open than that for clathrate hydrates and Dianin's compounds, which have been investigated previously. This factor allows us to probe the role of guest–host interactions in the determination of thermal properties of clathrates. The questions answered here are: How does the guest affect the anharmonicity of the HPTB lattice? How does the molecular setting influence the (guest and host) contributions to the intramolecular dynamics? Can the intramolecular modes of the clathrate be

reasonably approximated as sums of the guest and host modes? In what frequency range(s) do the dominant internal and external vibrational modes lie? How do these frequencies compare with those of the acoustic modes of the lattice? The latter two questions are particularly pertinent to laying a basis for understanding heat conduction in these materials.

Table 1. Smoothed values of the heat capacity at constant pressure, C_P, and heat capacity at constant volume, C_V, for HPTB. ($R = 8.31451$ J K^{-1} mol^{-1}.)

T (K)	C_P/R	C_V/R
30	11.6	11.6
35	14.3	14.2
40	16.7	16.6
45	19.0	18.9
50	21.1	21.0
60	25.0	24.7
70	28.4	28.1
80	31.6	31.1
90	34.5	33.8
100	37.3	36.4
120	42.7	41.5
140	48.1	46.5
160	53.6	51.7
180	59.3	57.2
200	65.1	62.8
220	71.0	68.4
240	76.8	74.1
260	82.6	79.5
280	88.2	84.8
300	94.0	90.0

2. Experimental procedure

The HPTB was prepared by a literature route [19]. Crystallization of this compound from the appropriate solution yields either a molecular crystal of HPTB or its particular clathrate.

Pure HPTB was recrystallized from chloroform by slow evaporation. It crystallizes in the triclinic $P\bar{1}$ space group with one molecule per unit cell ($a = 9.589(2)$ Å, $b = 10.256(1)$ Å, $c = 10.645(2)$ Å, $\alpha = 68.42(1)^\circ$, $\beta = 76.92(2)^\circ$, $\gamma = 65.52(1)^\circ$; $T = 18$ °C) [20]. The HPTB molecule is highly symmetrical in the solid state; phenyl groups are situated alternately above and below the plane of the central phenyl ring [20]. The packing coefficient, i.e. the ratio of the van der Waals volume of the molecular content of the unit cell to the volume of the unit cell itself determined by molecular mechanics [21], is 0.60. Organic molecular crystals typically have packing coefficients in the range 0.65 to 0.77 [22]. This low value of the packing coefficient, stemming from very open topology of the HPTB molecule, is one of the reasons for which this compound yields clathrates. The melting point of HPTB, as characterized by differential scanning calorimetry, was 180 °C [17].

Crystals of the CBr_4 clathrate of HPTB were grown from a solution of HPTB in chloroform with excess CBr_4 (3:1, CBr_4-to-HPTB mole ratio) by slow evaporation. The CBr_4 clathrate of HPTB crystallizes in a trigonal crystal system, with space group $R\bar{3}(h)$ ($a = 14.327(4)$ Å, $c = 20.666(8)$ Å; $T = 18$ °C) [20]. Its structure consists of a cavity in

the zone of the crystallographic *c*-axis, formed by eight host HPTB molecules. The guest molecules close the top and the bottom of the cage. The effective length of the cavity, which is occupied by two guest molecules, is $\simeq$17 Å. The gaps in the cage wall (determined from van der Waals radii and molecular mechanics [21]) are smaller than the effective sizes of the guest molecules. The enclathrated guests are oriented such that a C–Br bond of the CBr_4 molecule is along the threefold axis. There are three host and six guest molecules in the unit cell; density measurements [20] show 98% guest occupancy. HPTB $\cdot$ $2CBr_4$ melts incongruently at an onset temperature of 165.5 °C [17].

The heat capacities of HPTB and the CBr_4 clathrate of HPTB were measured in an adiabatic heat-pulse calorimeter. The apparatus and the procedure have been described in detail elsewhere [23, 24]. Briefly, this method is based on the measurement of the absolute value of the total heat capacity of the sample and the sealed calorimetric vessel through the determination of the temperature increment in response to energy provided to the system while maintaining adiabatic conditions. Knowledge of the predetermined heat capacity of the empty sample vessel as a function of temperature allowed the heat capacity of the sample to be determined. Previous measurements of the heat capacity of Calorimetric Conference (NBS-49) benzoic acid agreed with published values [25] to within 0.5% for the apparatus.

Raman spectra of powdered samples of HPTB and HPTB $\cdot$ $2CBr_4$ were obtained at 20 °C on a Bruker RFS 100 Fourier-transform Raman spectrometer. The laser (wavelength 1064 nm; linewidth less than 0.3 nm) was used at powers of up to 120 mW at the sample. A focused beam (180° geometry) was used. The spectral resolution was 4 cm^{-1}.

3. Results and discussion

3.1. Experimental findings

The heat capacities of HPTB and HPTB $\cdot$ $2CBr_4$ were measured in the temperature range from 30 K to 312 K (127 points) and from 30 K to 285 K (145 points), respectively. The heat capacity of the sample with respect to the heat capacity of the calorimeter varied with (increasing) temperature from 40% to 30% for pure HPTB and from 60% to 35% for the CBr_4 clathrate of HPTB. The relaxation times after heating did not exceed ten minutes in either compound, and for both compounds the relaxation times were slightly decreased at lower temperatures. No thermal history effects, which can indicate properties such as frozen disorder, were observed.

The observed heat capacities of HPTB and HPTB $\cdot$ $2CBr_4$ are shown in figure 3. Heat capacities of both compounds are smooth over the observed temperature range, with no singularities due to phase transitions. Smoothed values of the heat capacities for HPTB and HPTB $\cdot$ $2CBr_4$ are given in tables 1 and 2, respectively. The raw heat capacity data are available elsewhere [26].

The observed Raman spectra of HPTB and HPTB $\cdot$ $2CBr_4$ are shown in figures 4 and 5, respectively.

3.2. Isochoric heat capacity

The most useful thermodynamic variable related to the thermal properties of solid phases is the heat capacity at constant volume, C_V, which differs slightly from the experimentally determined quantity. The heat capacities measured were those under saturated vapour

Table 2. Smoothed values of heat capacity at constant pressure, C_P, and heat capacity at constant volume, C_V, for HPTB · 2CBr$_4$. ($R = 8.31451$ J K^{-1} mol^{-1}.)

T (K)	C_P/R	C_V/R
30	26.1	26.1
35	29.5	29.4
40	32.6	32.5
45	35.5	35.3
50	38.3	38.1
60	43.5	43.2
70	48.1	47.7
80	52.2	51.6
90	56.0	55.3
100	59.6	58.7
120	66.1	64.9
140	72.3	70.9
160	78.4	76.7
180	84.7	82.7
200	91.4	89.1
220	98.3	95.6
240	105.4	102.1
260	112.6	108.5
280	119.3	114.0
300	125.2	118.2

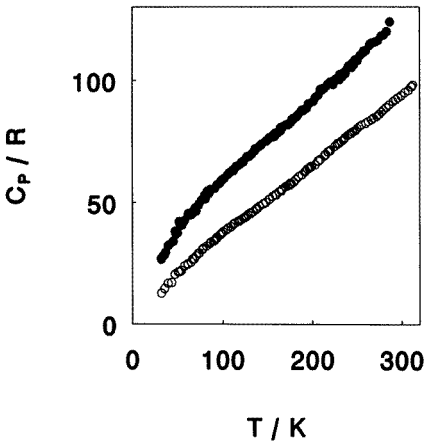

Figure 3. Experimental molar isobaric heat capacities, C_P, of HPTB (○) and HPTB · 2CBr$_4$ (●), with the latter expressed per mole of HPTB.

pressure, i.e. C_{sat}, which is related to the heat capacity at constant pressure, C_P, by [27]

$$C_{sat} = C_P - T\left(\frac{\partial P}{\partial T}\right)_{sat}\left(\frac{\partial V}{\partial T}\right)_P \tag{1}$$

where, for non-volatile solids, as here, $C_{sat} \simeq C_P$. The isobaric heat capacity is related to the isochoric heat capacity, C_V, through the general relation [27]

$$C_P - C_V = VT\left(c^T_{ijkl}\alpha_{ij}\alpha_{kj}\right) \tag{2}$$

where c^T_{ijkl} is the isothermal elastic constant tensor and α_{ij} is the thermal expansion tensor.

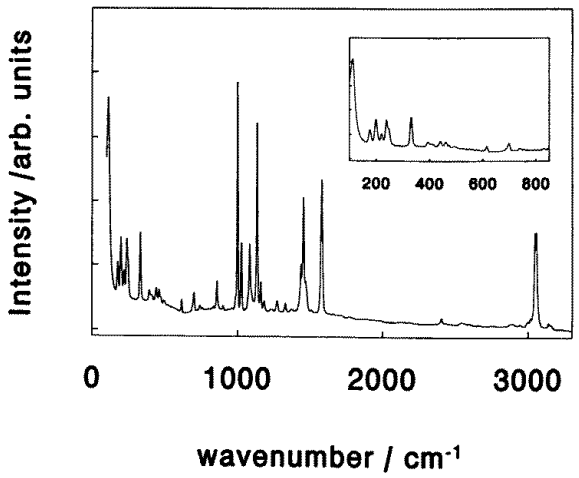

Figure 4. The observed room-temperature Raman spectrum of HPTB.

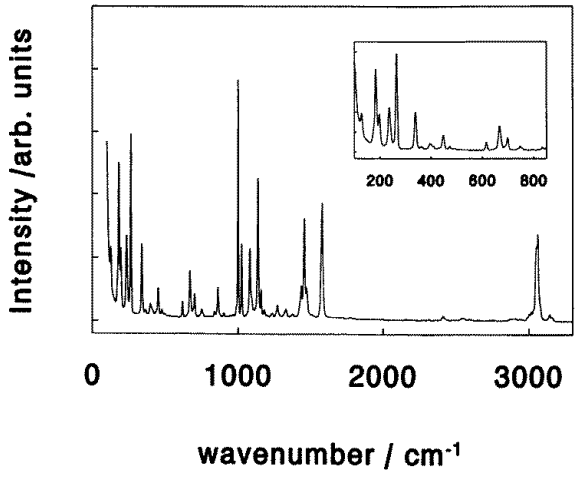

Figure 5. The observed room-temperature Raman spectrum of HPTB · $2CBr_4$.

We assume that $C_V \approx C_t$, where C_t is the heat capacity at constant strain.

For HPTB · $2CBr_4$, the elastic constants [28] and thermal expansion tensor [20] are known; for its trigonal structure, equation (2) reduces to

$$C_P - C_V = VT\left[2(c_{11} + c_{12})\alpha_a^2 + 4c_{13}\alpha_a\alpha_c + c_{33}\alpha_c^2\right] \tag{3}$$

and C_V can be derived from the experimental heat capacity values. Smoothed values of C_V for HPTB · $2CBr_4$ are listed in table 2.

Although the thermal expansion is known [20], the elastic constants of HPTB are not available for a similar (anisotropic) calculation of C_V. However, assuming that the isothermal compressibility, χ^T, for HPTB is similar to that found [28] for HPTB · $2CBr_4$,

we have calculated C_V for HPTB based on the isotropic equation:

$$C_P - C_V = \frac{V\alpha_V^2 T}{\chi^T} \tag{4}$$

where α_V is the volume thermal expansion of HPTB. The smoothed values of C_V for HPTB are given in table 1†.

With values of C_V for HPTB and HPTB · $2CBr_4$, we can now proceed to consider the various contributions to the heat capacity in these materials. Of particular interest is the additivity of the guest and host contributions, and it is in this matter that the Raman results are very useful.

3.3. Guest–host additivity

The Raman results provide an answer to the important question of how well represented the thermodynamic properties of HPTB · $2CBr_4$ are as the sums of those of HPTB and CBr_4.

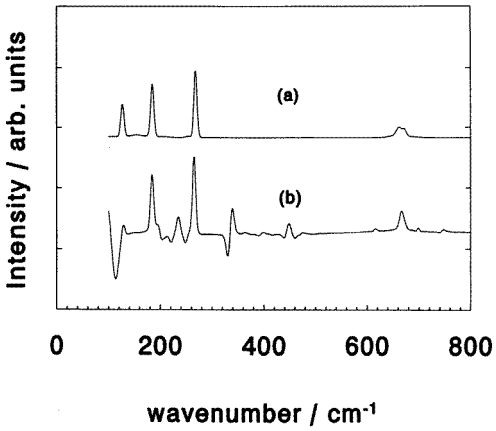

Figure 6. (a) The Raman spectrum of pure CBr_4; (b) the difference Raman spectrum, HPTB · $2CBr_4$ − HPTB.

The Raman difference spectrum (HPTB · $2CBr_4$ − HPTB; see figure 6(b)) shows that many of the features of the Raman spectra are the same for HPTB and HPTB · $2CBr_4$. Where they are exactly the same, the difference spectrum is flat, and where there are minor differences in frequency between features in HPTB and HPTB · $2CBr_4$, a positive peak (a feature present only in HPTB · $2CBr_4$) is found immediately adjacent to a negative peak (a feature present only in HPTB). Above 800 cm^{-1}, the only features are positive peaks within about 4 cm^{-1} (the spectral resolution) of negative peaks. This indicates that the high-frequency Raman-active modes of HPTB are essentially the same in HPTB · $2CBr_4$.

At lower wavenumbers, there are some distinct differences between the Raman spectra of HPTB and HPTB·$2CBr_4$, as seen in figure 6. The HPTB·$2CBr_4$−HPTB difference spectrum is shown in comparison with the Raman spectrum of pure solid CBr_4 (Aldrich, 99%, used without further purification; Raman spectra taken under same conditions as for HPTB and

† A recent lattice dynamical calculation [48] shows the compressibility of HPTB to be 8.9×10^{-11} m^2 N^{-1}, compared with 1.6×10^{-10} m^2 N^{-1} measured [28] for HPTB · $2CBr_4$. Use of this value of χ^T could lower the calculated value of C_V for HPTB (table 1) by about 4% at $T = 300$ K.

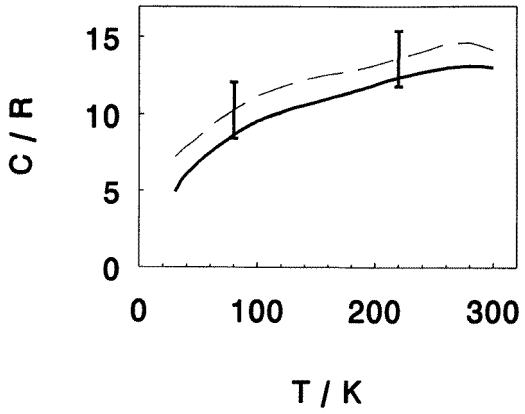

Figure 7. The molar isochoric heat capacities, C_V, for the CBr_4 molecule as a function of temperature for bulk CBr_4 (from [34], ——), and as determined by the difference between the heat capacity of HPTB · $2CBr_4$ and HPTB (- - - -). Propagation of a ±0.5% uncertainty in the total (sample + calorimeter) heat capacity of HPTB and HPTB · $2CBr_4$ gives an uncertainty denoted by the error bars shown.

HPTB · $2CBr_4$). The Raman spectrum of pure CBr_4 has been assigned [29], and this is of considerable help in understanding the features observed in the HPTB · $2CBr_4$ − HPTB difference spectrum: the features at 666, 265 and 183 cm^{-1} correspond, respectively, to modes ν_3, ν_1 and ν_4 of CBr_4 guest molecules. These CBr_4 modes in HPTB · $2CBr_4$ are all within a few cm^{-1} of the modes in pure CBr_4; the major difference is that ν_3, which we observe as a doublet in pure CBr_4, collapses to a single frequency in HPTB · $2CBr_4$, which suggests that the environment around the CBr_4 molecule in the clathrate is more isotropic than in pure (phase II) CBr_4. The remaining CBr_4 internal mode, ν_2, which occurs at 127 cm^{-1} in pure CBr_4, is present in HPTB · $2CBr_4$ (figure 5), but not so apparent in the HPTB · $2CBr_4$ − HPTB difference spectrum (figure 6(b)) due to other intense HPTB features in this region.

Altogether, the Raman results show that the internal vibrational modes (above 100 cm^{-1}) of the HPTB host molecules and the CBr_4 guest molecules are not greatly perturbed on going from the molecular solid to the CBr_4 inclusion compound, i.e. there is only a weak interaction between the CBr_4 internal motions and the environment. This conclusion complements results from IR difference spectra for several clathrates [30] and results from inelastic neutron scattering for Dianin clathrates [31]; the sum of these results shows the extraordinary utility of inclusion compounds in probing intermolecular interactions.

Furthermore, especially given the dominance of internal modes (*vide infra*), the Raman results for HPTB and HPTB · $2CBr_4$ show that the heat capacity of HPTB · $2CBr_4$ can be well represented as the sum of those of HPTB and CBr_4. This will be useful in the discussion to follow.

3.4. The heat capacity of a CBr_4 guest in HPTB · $2CBr_4$

On the basis of the Raman results for HPTB and HPTB · $2CBr_4$, which show the internal modes of the host and guest molecules to be nearly the same in the molecular solid and the clathrate, we can assume additivity of the host and guest contributions to the total heat capacity of HPTB · $2CBr_4$. In doing so, using the C_V-values, we have determined, by finding

the difference, the contribution of the CBr_4 guest to C_V. A similar approach was taken in the cases of quinol systems [32], THF clathrate hydrate [14] and Dianin's systems [33]. For the latter the heat capacity of the host lattice was measured directly since the clathrand of this compound exists, whereas the heat capacity of the empty quinol host lattice was extrapolated from the heat capacity of clathrates with different guest concentrations. For HPTB · $2CBr_4$ the situation is analogous to that of THF clathrate hydrate: the clathrand does not exist and there are no data available to extract the heat capacity of the empty host lattice from, since the clathrates of HPTB seem to have fixed compositions. Thus the heat capacity of pure HPTB was used as the only feasible approximation for the empty host framework of HPTB · $2CBr_4$, and this approximation is supported by the Raman results.

The 'molecular', i.e. guest, heat capacity of CBr_4 is shown in figure 7, in comparison with the heat capacity of pure CBr_4 [34]. Within the uncertainty shown in the figure, the heat capacity of the CBr_4 guest is essentially the same as that for bulk CBr_4, from 35 K to 300 K.

From an analysis of the heat capacity of pure CBr_4 it was found [34] that the contributions due to low-frequency translation and rotational vibrations of the rigid CBr_4 molecules are virtually fully excited at very low temperatures ($\simeq$45 K), and the temperature dependence of the heat capacity in the observed temperature range (30 to 305 K) is due to thermal excitation of internal degrees of freedom. The contributions of the heat capacity of the CBr_4 guest in HPTB · $2CBr_4$ can be considered to be similar, on the basis of the heat capacities shown in figure 7 and the additivity of the Raman spectra.

3.5. Contributions to the heat capacities of HPTB and HPTB · 2CBr$_4$

3.5.1. HPTB. The contribution to the total heat capacity of a molecular crystal comes from the internal and external modes, as described by the Born–von Kármán formalism of lattice dynamics. For HPTB (78 atoms per molecule), there are $3 \times 78 - 6 = 228$ internal-mode optical branches to the phonon dispersion and 6 external branches (3 acoustic, 3 optic).

The internal modes could be assessed via Einstein-like contributions of the optic modes, except that only 71 of the possible 228 modes are observed in the present Raman experiment. The reduced number of observed modes is undoubtedly related to degeneracy, especially given the relatively high symmetry of the molecule. By similarity with other hexasubstituted benzenes and thiols [35, 36], it is likely that the features in the range of 1000 cm^{-1} correspond to breathing vibration(s), those in the 600–700 cm^{-1} range correspond to C–S motions, those in the range 600–3000 cm^{-1} correspond to planar vibrations of the phenyl rings, and those below 300 cm^{-1} correspond to phenyl librations. Although we have not assigned the spectrum, it is important for further discussion (*vide infra*) that we realize the high probability of degeneracy in the features throughout the observed Raman range ($<$3300 cm^{-1}). As a first approximation, we can consider the 71 observed modes to be equally degenerate, i.e. each weighted by 228/71 in the calculation of the internal-mode contribution to the heat capacity.

Based on the information for HPTB · $2CBr_4$ (*vide infra*), the acoustic modes were approximately represented by a Debye characteristic temperature of 87 K. Given that the rigid-molecule librations of a molecular crystal can be expected to occur at a relatively low frequency (for example, this was found [37] to be 32 cm^{-1} for C_{60}), this contribution was calculated here with an Einstein model in which the characteristic frequency was chosen to be 50 cm^{-1}. The latter was a somewhat arbitrary choice, but the small contribution of the acoustic modes and the whole-molecule librational modes to the total heat capacity of HPTB makes the absence of quantitative information concerning these frequencies less

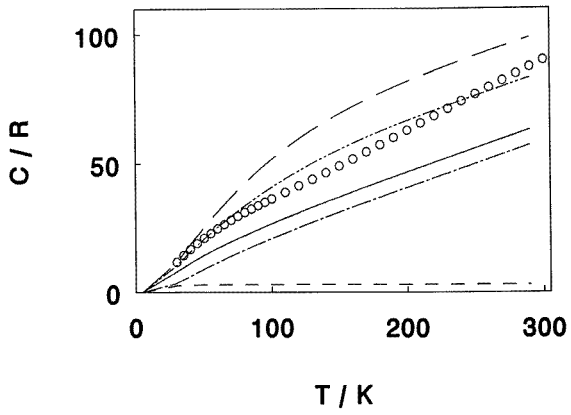

Figure 8. Contributions to the heat capacity, C, of HPTB as a function of temperature: - - - -, acoustic modes; – – –, internal modes of HPTB (equally weighted); ——, calculated C_V(total) considering equal weighting of HPTB internal modes; – - - – - -, calculated C_V(total) considering double weighting of HPTB internal modes at <400 cm^{-1}; — — —, calculated C_V(total) considering triple weighting of HPTB internal modes at <400 cm^{-1}; ○, C_V derived from experiment.

serious than it might otherwise be.

The total heat capacity of HPTB, based on the above calculations, is shown in figure 8 in comparison with the C_V-values of HPTB from table 1. From the figure it can be seen that the total heat capacity falls short of the experimental C_V throughout the entire temperature range of the experiment. Since adjustment of the Debye temperature or the whole-molecule librational frequency will do little to change this outcome, the main source of discrepancy must be the 'equal-weight' assignment of the observed internal optic modes. In order to increase the calculated C_V, the lowest-frequency modes must be weighted more than the higher-frequency modes. The effects of increasing the contribution of the modes at less than 400 cm^{-1}, to double and triple the contribution of those modes >400 cm^{-1}, are shown in figure 8. (The value of 400 cm^{-1} was chosen for these calculations as we are most concerned with modes that are substantially excited at room temperature, and at $T = 300$ K a mode at 400 cm^{-1} has achieved 75% of the maximum value of its heat capacity.)

3.5.2. HPTB · 2CBr$_4$. Contributions to the heat capacity of HPTB · 2CBr$_4$ arise from both the host and the guest. On the basis of the Raman results, we consider these contributions separately.

One contribution of the heat capacity of the CBr$_4$ molecules results from internal motions ($3 \times 5 - 6 = 9$ degrees of freedom), described by the Einstein model and calculated here using the Raman frequencies associated with the CBr$_4$ guest molecules; the degeneracies are as assigned for bulk CBr$_4$ [29]. Another contribution of the CBr$_4$ molecules is their rigid-molecule libration; using the results of x-ray diffraction [20] and the method of Cruickshank [38], we find this mode to be at about 30 cm^{-1}, and its contribution to the heat capacity has been calculated from a three-dimensional Einstein model.

As for pure HPTB, the internal motions of the HPTB molecule contribute $3 \times 78 - 6 =$ 228 degrees of freedom, but fewer (99) lines are observed in the Raman spectrum (<3300 cm^{-1}). Considering these to be equally weighted (i.e. an effective degeneracy of 228/99), their Einstein contributions to the heat capacity have been calculated. In addition

to the internal degrees of freedom, the contribution of the rigid-molecule libration of HPTB to the heat capacity has been approximated as a three-dimensional Einstein oscillator of characteristic frequency 50 cm^{-1}.

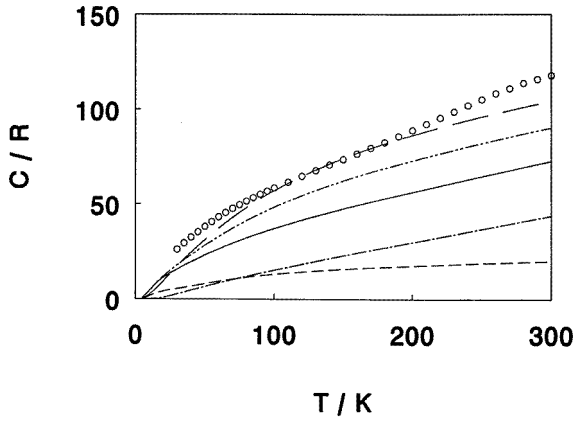

Figure 9. Contributions to the heat capacity, C, of HPTB · $2CBr_4$ as a function of temperature: - - - -, the contribution of internal and librational modes of CBr_4; – – –, internal modes of HPTB (equally weighted); ——, calculated C_V(total) considering equal weighting of HPTB internal modes; – - - – - -, calculated C_V(total) considering double weighting of HPTB internal modes at <400 cm^{-1}; — — —, calculated C_V(total) considering triple weighting of HPTB internal modes at <400 cm^{-1}; ○, C_V derived from experiment.

In order to complete the degrees of freedom of the system, we must include the acoustic modes. There is too much uncertainty (*vide infra*) in the dominating contribution of the internal degrees of freedom to determine the Debye characteristic temperature from the present calorimetric data (i.e. by subtraction of the contribution of the internal modes to the low-temperature heat capacity). However, Θ_D^{el}, the characteristic temperature from the elastic data, can be assessed from the following expression [39]:

$$\Theta_D^{el} = \frac{h v_m}{k_b} \left(\frac{3 N_A n \rho}{4 \pi M} \right)^{1/3} \tag{5}$$

where h, k_B and N_A are the Planck, Boltzmann and Avogadro constants, respectively, ρ is the density of HPTB · $2CBr_4$ (from [20]), M is the molecular mass, and v_m is the mean phonon speed ($= (3)^{1/3}(v_L^{-3} + 2v_T^{-3})^{-1/3}$), where v_L and v_T are the longitudinal and transverse speeds, respectively, which, for an isotropic trigonal system, are given by [40] $v_L^2 = c_{33}/\rho$ and $v_L^2 = c_{44}/\rho$. (Strictly speaking, this system is anisotropic [28].) The elastic constants, c_{33} and c_{44}, are known [28] for HPTB · $2CBr_4$. The parameter n in equation (5) is the number of loosely associated groups (or, equivalently, non-rigorously defined sites in the unit cell; these sites correspond to atomic positions in an atomic crystal); we have taken $n = 11$ here (four for the CBr_4 guests and seven for HPTB). On this basis, we find Θ_D^{el} for HPTB · $2CBr_4$ to be 87 K, and calculate the acoustic contribution to the heat capacity as 11 three-dimensional Debye modes with $\Theta_D = 87$ K, completing the 264 degrees of freedom. The total calculated heat capacity and several of its components are shown in figure 9.

As for HPTB, the calculated heat capacity falls below the observed heat capacity. Again, the major uncertainty in the calculation is the degeneracy of the internal degrees of freedom of HPTB, and, in order for the calculated heat capacity to be increased, the low-frequency modes must be weighted more than the higher-frequency modes. For illustration,

double and triple weightings of the modes in the range 100 to 400 cm^{-1} (at the expense of the modes >400 cm^{-1}) are shown in figure 9; although the latter helps somewhat, there is still considerable difference from the experimental heat capacity for both HPTB and HPTB $\cdot$ $2CBr_4$.

3.6. Grüneisen parameters

Intermolecular forces determine many properties of molecular crystals, particularly thermal and mechanical properties, since they define the character of the potential between the chemical species building a crystal. Knowledge of the spatial as well as the harmonic/anharmonic character of the intermolecular interaction is crucial in understanding lattice dynamics. The Grüneisen parameter has been a useful quantity for discussion of the anharmonic properties of solids, especially those displaying significant long-range interactions, such as ionic crystals. To date, Grüneisen parameters of molecular crystals have not been investigated so extensively. Thus we turn our attention to anharmonic properties of HPTB and HPTB $\cdot$ $2CBr_4$ since relevant values of the thermal properties are available to quantify these.

It is reasonable to assume that the value of the adiabatic compressibility of HPTB (no experimental values are available) will be comparable to that of the clathrate [28]. By virtue of this premise the overall Grüneisen parameter was determined for pure HPTB from the relation

$$\gamma = \frac{\alpha_V V}{\beta_T C_V} \left(= \frac{\alpha_V V}{\beta_S C_P} \right) \tag{6}$$

where α_V is the HPTB thermal volume expansion [20] and $\beta_{T\,(S)}$ is its isothermal (adiabatic) compressibility [28].

In the case of HPTB $\cdot$ $2CBr_4$ relevant tensors are known [28, 20], and it is possible to apply the anisotropic version of equation (6). For axial systems there are only two non-zero independent directional Grüneisen parameters [41]:

$$\gamma_a \ (= \gamma_b) = (V/C_\sigma)((c_{11} + c_{12})\alpha_a + c_{13}\alpha_c) \tag{7}$$

$$\gamma_c = (V/C_\sigma)(2c_{13}\alpha_a + c_{33}\alpha_c) \tag{8}$$

where c_{ij} are the adiabatic elastic constants and C_σ is the heat capacity at constant stress ($\approx C_P$). Since the volume thermal expansion is a combination of α_a and α_c, one can express the bulk Grüneisen parameter as [41]

$$\gamma = (2\beta_a\gamma_a + \beta_c\gamma_c)/\beta \tag{9}$$

where β_a and β_c are the linear adiabatic compressibilities along the a- and c-axes, respectively.

Plots of the bulk Grüneisen parameters for HPTB and HPTB $\cdot$ $2CBr_4$ are shown in figure 10. The directional Grüneisen parameters for HPTB $\cdot$ $2CBr_4$ are shown in figure 11. (The uncertainty in the HPTB compressibility does not affect the temperature dependence of the Grüneisen parameter, especially its elevation at lower temperatures, since the compressibility is nearly independent of temperature.)

The values of γ found here are comparable to those characteristic for non-metallic solids, $\gamma \approx 1$ [41]. The low-temperature increase of the Grüneisen parameter reflects the high thermal expansion at low temperature [20]. Although this is not typical because for most materials γ decreases with decreasing temperature [41], the same trend was observed for Dianin's compound and its clathrates [42], tetrahydrofuran hydrate [43], disordered materials and crystals doped with impurities [41]. In solid CO this elevation was attributed to the

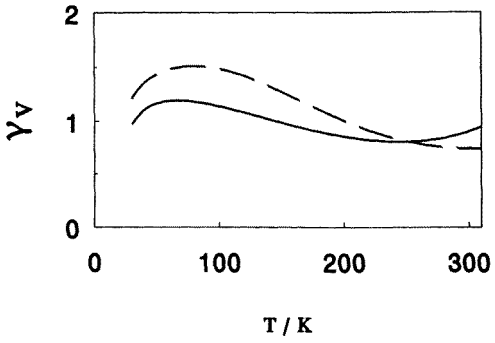

Figure 10. Bulk Grüneisen parameters, γ, as functions of temperature for HPTB (- - - -) and HPTB · $2CBr_4$ (——).

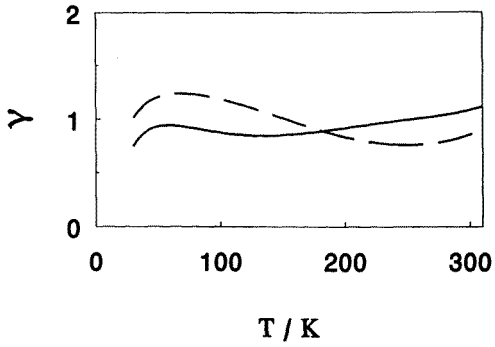

Figure 11. Directional Grüneisen parameters, γ_a (- - - -) and γ_c (——), for HPTB · $2CBr_4$ as functions of temperature.

presence of low-frequency librational modes [41]; our present heat capacity analysis shows the importance of low-frequency modes in both HPTB and HPTB · $2CBr_4$. In amorphous materials high γ-values were partially attributed to the linear temperature dependence of the heat capacity [41]; although the heat capacities of HPTB and HPTB · $2CBr_4$ are not quite linear, these materials have a wide range of frequencies due to internal vibrations, which lead to the heat capacities increasing monotonically with increasing temperature.

Assuming that for clathrates of a particular host compound, thermodynamical variables such as V, C_V and β are very similar at a given temperature (this is certainly true in Dianin's system [42]), equation (6) shows that the Grüneisen parameter is directly responsible for any differences between thermal expansivities of different clathrates. These findings can be put in the wider context of results for other clathrates. In contrast with HPTB, the clathrate hydrates and Dianin's systems exhibit enhanced thermal expansion for the clathrate with respect to the host compound (i.e. ice or the clathrand of Dianin's compound) [43, 44]. For the clathrate hydrates a phenomenological explanation was proposed [43]: increased thermal expansivity was attributed to weakened interactions between the water molecules of the host lattice due to pressure, ascribed to the kinetic motion of the guest molecules, exerted on the walls of cavities. It would seem even more reasonable to assume the same mechanism for Dianin's system, where guests experience motion within the molecular field of the crystal

and the character of this motion is less restrained than that of bonded chemical species or even molecular clusters. On the other hand, it has been shown that thermal expansion can be viewed as a response to the change in the dynamical internal pressure which is equivalent to the radiation pressure of the elastic waves on crystal walls [45]. Since in the clathrate hydrates and in Dianin's system the guests introduce additional motion (in comparison to the lattice of the pure host compound) the dynamical internal pressure is higher and therefore the thermal expansivity is higher. It could be concluded that the reduced thermal expansivity of HPTB · $2CBr_4$ relative to HPTB [20] might stem from differences between their structures (HPTB is a molecular solid and HPTB · $2CBr_4$ is a clathrate) and those of the clathrate hydrates and Dianin's clathrates. All three systems conform to the topological definition of a clathrate compound, i.e. a structure based on lattice lacunae. Yet a subtle, but most significant, distinction lies in the constitution of these assemblies. Dianin's clathrate and clathrate hydrates form well defined cavities: the clathrate edifice is composed of the host molecules associated through hydrogen bonds, and the steric barriers which limit the volume of the voids are tight. This lets the guests have noticeable impact on the thermal expansion. In contrast, the HPTB clathrates are more open. Two supramolecular hexamers close the cage tightly in the Dianin's assemblies; the cavity in HPTB clathrate is created by eight host molecules. This also indicates the crucial role of intermolecular interactions and their directional dependence: despite the remarkable resemblance between the supramolecular unit of Dianin's compound and the molecular structure of HPTB, their clathrates exhibit quite different host lattice topologies. The guests in HPTB can be considered as space fillers that are loosely retained in the lattice. This also explains why some guests such as CCl_4 or CH_3CCl_3 are easily lost from HPTB. In essence, the guest in HPTB does not increase the pressure on the host lattice as in Dianin's system and in clathrate hydrates, and hence the Grüneisen parameter of HPTB · $2CBr_4$ is less than that of pure HPTB.

Before concluding the discussion of the Grüneisen parameters, we draw attention to the possible effect of coupling between internal and external modes on the Grüneisen parameter and its reflection of the anharmonicity of the crystal lattice potential [41, 46, 34, 47]. Since the internal modes and external modes overlap in frequency range for HPTB and HPTB · $2CBr_4$, the temperature evolution of the calculated γs could be influenced by mode coupling.

4. Conclusions

From calculation of the heat capacities of HPTB and HPTB · $2CBr_4$, in comparison with the measured heat capacities, we find that low-frequency modes play a dominant role, despite the wide range of frequencies associated with intramolecular vibrations in both compounds. We based these calculations on the additivity of guest and host contributions to the heat capacity, which, from the Raman spectroscopic results, we find to be a reasonable premise despite the major differences in structure between HPTB and HPTB · $2CBr_4$.

The calculated Grüneisen parameters are higher for HPTB than HPTB · $2CBr_4$. This is consistent with the dominance of low-frequency modes in this rather open molecular crystal.

Acknowledgments

This work was supported by the Natural Sciences and Engineering Research Council of Canada (grants to MAW and a scholarship to DM); DM also held a Killam Memorial Scholarship.

References

[1] MacNicol D D, McKendrick J J and Wilson D R 1978 *Chem. Soc. Rev.* **7** 61
[2] Weber E and Josel H-P 1983 *J. Inclusion Phenom.* **1** 79
[3] Powell H M 1948 *J. Chem. Soc.* 61
[4] Powell H M 1984 *Inclusion Compounds* vol 1, ed J L Atwood, J E D Davies and D D MacNicol (London: Academic) p 1
[5] van der Waals J H 1956 *Trans. Faraday Soc.* **52** 184
[6] van der Waals J H 1959 *Advances in Chemical Physics* ed I Prigigone (New York: Interscience) p 1
[7] Belosludov V R, Lavrentiev M Yu and Dyadin A Yu 1991 *J. Inclusion Phenom.* **10** 399
[8] Rodger P M 1990 *Mol. Simul.* **5** 315
[9] Rodger P M 1990 *J. Phys. Chem.* **94** 6080
[10] Lynden-Bell R M 1993 *Mol. Phys.* **79** 313
[11] Stoll R D and Bryan G M 1979 *J. Geophys. Res.* **84** 1629
[12] Ross R G, Andersson P and Bäckström G 1981 *Nature* **290** 322
[13] Cook J G and Leaist D J 1983 *Geophys. Res. Lett.* **10** 397
[14] White M A 1987 *J. Physique Coll.* **48** C1 565
[15] Zakrzewski M and White M A 1992 *Phys. Rev.* B **45** 2809
[16] Michalski D and White M A 1995 *J. Phys. Chem.* **99** 3774
[17] White M A and Perry R T 1994 *Chem. Mater.* **6** 603
[18] MacNicol D D and Wilson D R 1976 *J. Chem. Soc. Chem. Commun.* 494
[19] Hardy A D, MacNicol D D and Wilson D R 1979 *J. Chem. Soc. Perkin Trans.* **2** 1011
[20] Michalski D, White M A, Bakshi P K, Cameron T S and Swainson I 1995 *Can. J. Chem.* **73** 513
[21] *CHEM-X* 1990 Chemical Design Ltd, Oxford, UK
[22] Kitaigorodsky A I 1973 *Molecular Crystals and Molecules* (New York: Academic)
[23] White M A 1984 *Thermochim. Acta* **74** 55
[24] Van Oort M J M and White M A 1987 *Rev. Sci. Instrum.* **58** 1239
[25] Ginnings D C and Furukawa G T 1953 *J. Am. Chem. Soc.* **75** 522
[26] Michalski D 1995 *PhD Thesis* Dalhousie University, Halifax, Canada
[27] Wallace D C 1972 *Thermodynamics of Crystals* (New York: Wiley)
[28] Michalski D, Mróz B, Kiefte H, White M A and Clouter M J 1993 *J. Phys. Chem.* **97** 12 949
[29] Tse W S, Liang N T, Lin W W and Chiang P Y 1985 *Chem. Phys. Lett.* **119** 67
[30] Davies J E D 1985 *J. Inclusion Phenom.* **3** 269
[31] White M A, Powell B M and Sears V F 1992 *Mol. Cryst. Liq. Cryst.* **211** 177
[32] Parsonage N G and Staveley L A K 1959 *Mol. Phys.* **2** 212
[33] White M A and Zakrzewski M 1990 *J. Inclusion Phenom. Mol. Recog. Chem.* **8** 215
[34] Michalski D and White M A 1995 *J. Chem. Phys.* **103** 6173
[35] Lin-Vien D, Colthup N B, Fateley W G and Graselli J G 1991 *The Handbook of Infrared and Raman Characteristic Frequencies of Organic Molecules* (San Diego, CA: Academic)
[36] Dollish F R, Fateley W G and Bentley F F 1974 *Characteristic Raman Frequencies of Organic Compounds* (New York: Wiley)
[37] White M A, Meingast C, David W I F and Matsuo T 1995 *Solid State Commun.* **94** 481
[38] Cruickshank D W J 1958 *Rev. Mod. Phys.* **30** 163
[39] Anderson O L 1965 *Physical Acoustics* vol IIIB (New York: Academic) p 43
[40] Truell R, Elbaum C and Chick B B 1969 *Ultrasonic Methods in Solid State Physics* (New York: Academic) p 12
[41] Barron T H K, Collins J G and White G K 1980 *Adv. Phys.* **29** 618
[42] Zakrzewski M and White M A 1991 *J. Phys.: Condens. Matter* **3** 6703
[43] Tse J S 1987 *J. Physique Coll.* **48** C1 543
[44] Zakrzewski M, White M A and Abriel W 1990 *J. Phys. Chem.* **94** 2203
[45] Ceccaldi D, Ghelfenstein M and Szwarc H 1975 *J. Phys. C.: Solid State Phys.* **8** 417
[46] Zallen R 1974 *Phys. Rev.* B **9** 4485
[47] Chandrasekharan V, Farbre D, Thiery M M, Uzan E, Donkersloot M C A and Walmsley S H 1974 *Chem. Phys. Lett.* **26** 284
[48] Michalski D 1995 unpublished